Hardware-in-the-loop experimental setup for high-speed milling

G. Stepan[1], D. Takacs[2], R. Wohlfart[1], A. Miklos[2], G. Porempovics[1], A. Toth[3]

[1]Department of Applied Mechanics, Budapest University of Technology and Economics, Budapest, Hungary

[2]MTA-BME Research Group on Dynamics of Machines and Vehicles, Budapest, Hungary

[3] Department of Manufacturing Science and Engineering, Budapest University of Technology and Economics, Budapest, Hungary

Abstract

The hardware-in-the-loop experiment of high speed milling is introduced. The tool-workpiece interaction is implemented in the virtual part while the machine together with the spindle is the real element of the setup. Main tasks of the development of the HIL test are discussed. The prototype of a contactless sensor is presented by which the displacement of the rotating tool can be measured with high accuracy. A computational algorithm of the tool-workpiece interaction is constructed, and required computational efforts are estimated accurately. Finally, the development of a contactless electromagnetic actuator is presented, which can be used to generate the virtual cutting force.

Keywords:

hardware-in-the-loop, contactless sensor, electromagnetic actuator

1 INTRODUCTION

Theoretical analyses of the models of high speed milling processes aim to predict both the linear stability limits of cutting and the so-called unsafe parameter domains below the stability boundaries where chatter may still occur with certain probability. The industrial applications of these theoretical results are still limited by the availability of extensive laboratory tests required for the validation of the models in case of various working conditions and tool geometries, and also to explore the range of uncertainties of certain parameters. The cost of these tests can be reduced substantially by means of the emulation of the tool/workpiece interaction in so-called hardware-in-the-loop (HIL) experiments.

The reliability of HIL experiments strongly depends on the applied sampling frequency that can be used during the simulation of the cutting forces. For example, corresponding tests were carried out for stick-and-slip processes in [1] where the asymmetric nonlinearity of the Stribeck contact force is similar to that of the cutting force. One of the important conclusions is that the HIL experiments do not provide conservative estimates if the sampling time is larger than a critical value.

The goal of the research is related to the development of a HIL experimental setup for high-speed milling, which can also be considered as semi-virtual machining. The machine tool structure together with the tool, the spindle and its bearings are there physically, while the forces generated by the cutting process are emulated by actuators. The loop is closed by means of sensors that measure the displacements of the tool. The signals are processed in real time computation.

There are several challenges during the compilation of this project. The first task is the development of a contactless, large frequency bandwidth and high resolution direct displacement measuring system. The second task is the compilation of real-time computations with less than 0.01 ms cycle time with more than 6000 operation/cycle, which are set based on the first series of experiments. The third task is the construction of a contactless electromagnetic actuator that provides large enough forces that can vary with large frequency. The actual problems are related to the occurrence of eddy current and heat, and also to the high-frequency control of large currents.

In this presentation, the development of a HIL experiment is in focus. A custom built laser sensor and electro-magnetic actuator are presented. A computational algorithm is also shown, the implementation of which on high performance FPGA chip enables the emulation of the cutting force even for intricate tool geometries.

2 CONCEPT OF VIRTUAL MACHINING IN HIL

The concept of the HIL experiment is shown in Figure 1. Instead having the real milling tool in the spindle, a dummy tool is used. The spatial position of the tool is determined via the measured radial displacements of two cross-sections of the dummy tool, while the rotational position of the tool is detected by the encoder of the spindle. The torsional and longitudinal vibrations of the spindle are not taken into account in the experiment. The resultant cutting force is emulated on the dummy tool based on the real time computational algorithm; this way, complex virtual tool and workpiece geometries and material properties can be considered.

Three essential problems can be emphasized in connection with the HIL experiment:

- the contactless displacement measurement of the rotating tool,
- the real time computation of the cutting force,
- the emulation of the cutting force.

These topics are investigated and discussed in the following three subsections. The paper concludes with a section where the achieved results and the future plans are summarized briefly.

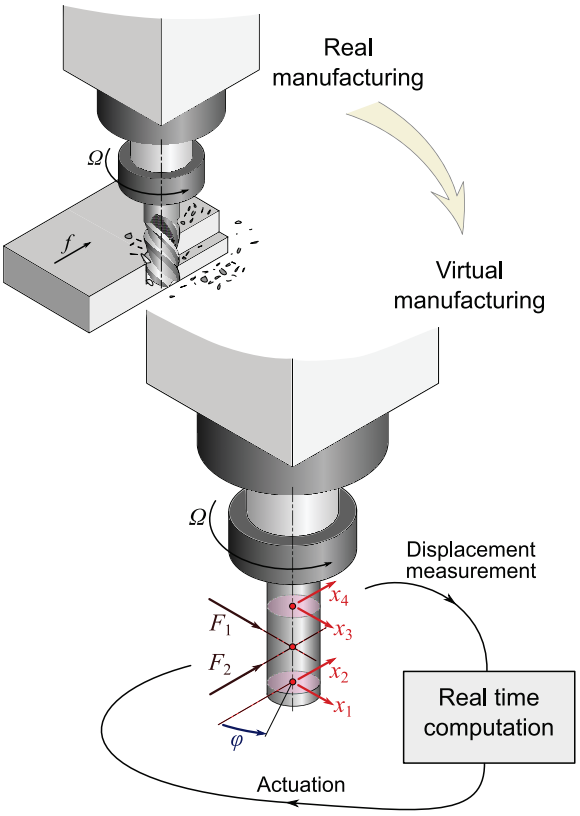

Figure 1: Concept of virtual machining in HIL test

3 DISPLACEMENT MEASUEREMENT OF THE ROTATING TOOL

To measure the position of the dummy tool, contactless displacement sensors are required. Contactless measurement is a classical task in the field of rotor dynamics as it is in the field of machine tool vibration detection. For example, to determine the theoretical stability charts of milling processes, natural frequencies, damping ratios of the vibration modes are needed. In most common cases, the frequency response function (FRF) of the tool side is measured with impact hammers and accelerometers attached to the tool tip. Of course, in this arrangement, the spindle cannot rotate. However, it is well known, that stiffness and damping parameters of angular contact bearings vary with the rotational speed, and the gyroscopic effect can also be relevant at high rotational speed (see [2]). To identify the variation of the parameters of the spindle with respect to the rotational speed, measurement has to be carried out meanwhile the spindle rotates.

One of the commonly used contactless measurement devices is the Laser-Doppler vibrometer, which provides the velocity of the measured target in the direction of the laser beam. To detect higher natural frequencies, this sensor can be useful since close to the resonance the vibration velocities are large enough. In the HIL test, where we are interested in a wide frequency range and the accurate displacements are essentially needed for the calculation of the cutting force, Laser-Doppler vibrometers are not useful. Reflective laser based displacement sensors are also available in the market (see in [3]) with different measuring range and resolution, but the frequency bandwidth of the reflective laser sensors is usually low, and their resolution is also limited.

In order to exploit all the advantageous properties of laser based sensors, a sensor was designed with very high resolution and frequency bandwidth. The basic idea of the developed Fotonic Beam Reduction (FBR) sensor is shown in Figure 2. A laser beam is tangentially directed to the dummy tool and the intensity of the laser beam is measured by a photodiode at the other side of the tool. If the tool moves in the transversal direction of the laser beam, the laser beam fades in/out – the width of the laser beam received by the photodiode is modulated – and the measured intensity increases/decreases. Thus, this type of contactless sensor can measure the displacement of the tool directly. The first prototype of the sensor is shown in Figure 3. It has 500 kHz frequency bandwidth, 10-100 nm resolution, 0.1-0.2 mm measuring range. The RMS noise level is below 10 nm, the sensitivity is around 10 mV/µm.

Displacement signals of a dummy tool with 16 mm diameter are shown in Figure 4. An impact-like perturbation was applied and the response was recorded at zero and at 8018 rpm spindle speed.

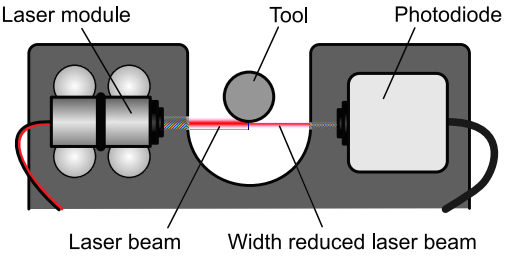

Figure 2: Concept of the FBR sensor

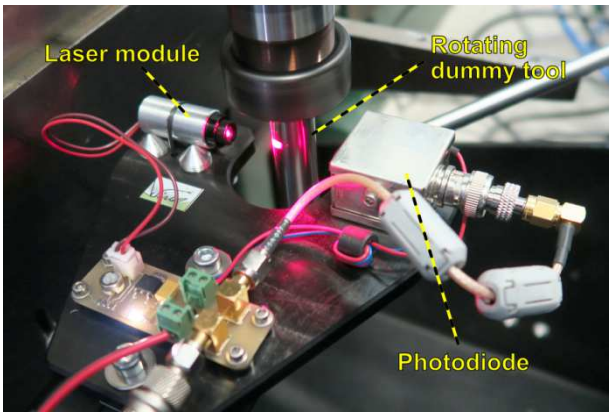

Figure 3: Prototype of the FBR sensor

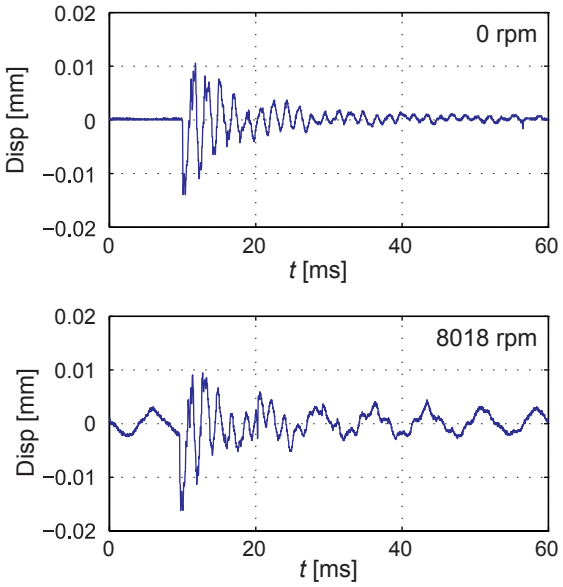

Figure 4: Time histories of the vibrations of the tool measured by the FBR sensor at zero and non-zero spindle speed

4 REAL TIME CALCULATION

In case of virtual machining, the cutting force generated by an actuator has to be calculated in the virtual part of the HIL experiment. In order to do this, we use the calculation method that is given in [3], where the linear stability analysis of milling is investigated for different tool geometries.

4.1 Computation algorithm

In the HIL test, we intend to apply the non-stationary part of the cutting force only, namely, we do not consider the stationary vibration of the tool caused by the stationary cutting force. This limitation is used because the applied actuator cannot generate large forces but it is designed with large frequency bandwidth. In the algorithm, when the cutting force is calculated, we consider that the non-stationary part of the cutting force depends linearly on the chip thickness. To determine the chip thickness, the actual position of the dummy tool is needed. Since the dummy tool is considered to be rigid (it is designed to be as stiff as possible) and its axial movement is neglected in the calculation, 5 state variables are required to describe its spatial position (see Figure 1), i.e. 5 input signals have to be measured and handled by the real target:

- 1 incremental encoder signal determining the rotational position $\varphi(t)$ of the spindle;
- 4 analogue signal $x_1(t), x_2(t), x_3(t)$ and $x_4(t)$ corresponding to the transversal positions of two cross sections of the dummy tool.

In the computational algorithm, the cutting force is determined and output signals are arranged based on the characteristics of the actuator. For our specific case, we require 4 analogue outputs to provide the desired current values $i_1(t), i_2(t), i_3(t)$ and $i_4(t)$ of the coils that generate the in-plane virtual cutting force in the actuator.

Based on the sampling frequency f of the input and output signals, the time increment can be introduced as

$$\Delta t = \frac{1}{f} \tag{1}$$

and the time is quantized as:

$$t_k = k\Delta t, \quad k = 0,1,2,\ldots. \tag{2}$$

This way, the input/output signals are discretized in time:

$$x_{i,k} \coloneqq x_i(t_k), \quad \varphi_k \coloneqq \varphi(t_k) \quad i_{j,k} \coloneqq i_j(t_k)\ . \tag{3}$$

In order to calculate the resultant cutting force, the following computation has to be accomplished:

$$F_{l,k+1} = \sum_{i=1}^{4} \mathbf{w}_{lir}^{\mathrm{T}} \hat{\mathbf{x}}_{i,k} \quad \text{for} \quad l = 1,2\ . \tag{4}$$

In this equation, the vectors are defined as

$$\hat{\mathbf{x}}_{i,k} = \begin{bmatrix} x_{i,k} & x_{i,k-n_\tau} & x_{i,k-2n_\tau} & \ldots & x_{i,k-Nn_\tau} \end{bmatrix}^{\mathrm{T}}, \quad i = 1,2,3,4, \tag{5}$$

the sizes of which are $(N+1)\times 1$. Consequently, these vectors contain the actual and the past values of the measured displacement signals. The value of n_τ can be calculated as

$$n_\tau = \mathrm{int}\left(\frac{T}{N\Delta t}\right), \quad \text{where} \quad N \le T/\Delta t \quad \Rightarrow \quad 1 \le n_\tau. \tag{6}$$

Here, T refers to the time period of one revolution of the spindle, namely,

$$T = \frac{2\pi}{\Omega}\ , \tag{7}$$

where Ω is the angular velocity of the spindle. All these mean that the number N specifies how many former values of measured displacement signals are used in the calculation of the cutting force. The larger N is, the more precise the consideration of the regenerative effect is. Hence, N can be thought of as the resolution of the time domain.

In (4), the notation $\mathbf{w}_{lir}$ refers to the constant vectors

$$\mathbf{w}_{lir} = \begin{bmatrix} w_{lir1} & w_{lir2} & \ldots\ldots & w_{lir(N+1)} \end{bmatrix}^{\mathrm{T}}, \tag{8}$$

with size are $(N+1)\times 1$, and the subscript r is determined based on the rotational position of the spindle, namely:

$$r = \mathrm{int}\left(\frac{\mathrm{mod}(\varphi_k, 2\pi)}{n_\varphi \Delta\varphi}\right) + 1 \tag{9}$$

with

$$n_\varphi = \frac{2\pi}{M\Delta\varphi}, \quad \text{where} \quad M \le 2\pi/\Delta\varphi \quad \Rightarrow \quad 1 \le n_\varphi. \tag{10}$$

The parameter M can be identified as a resolution that determines how many rotational positions of the tool are differentiated in the HIL test. The larger M is, the more precise the calculation is.

Vectors $\mathbf{w}_{lir}$ can be arranged into the matrices:

$$\mathbf{W}_{li} = \begin{bmatrix} \mathbf{w}_{li1} & \mathbf{w}_{li2} & \ldots & \mathbf{w}_{liM} \end{bmatrix}, \quad l = 1,2,\ i = 1,2,3,4. \tag{11}$$

The size of $\mathbf{W}_{li}$ is $(N+1)\times M$, and $2\times 4 = 8$ matrices are used for the calculation. These matrices can be loaded preliminarily into the memory of the real target computer based on the calculation method presented in [3].

The output signals, i.e. the desired currents of the coils in the actuator, can be calculated by means of the calculated virtual cutting force $F_{l,k+1}$, namely:

$$\begin{aligned}
i_{1,k+1} &= \begin{cases} f_1(F_{1,k+1}) & \text{if} \quad F_{1,k+1} > 0, \\ 0 & \text{if} \quad F_{1,k+1} \le 0, \end{cases} \\
i_{2,k+1} &= \begin{cases} f_2(F_{1,k+1}) & \text{if} \quad F_{1,k+1} < 0, \\ 0 & \text{if} \quad F_{1,k+1} \ge 0, \end{cases} \\
i_{3,k+1} &= \begin{cases} f_3(F_{2,k+1}) & \text{if} \quad F_{2,k+1} > 0, \\ 0 & \text{if} \quad F_{2,k+1} \le 0, \end{cases} \\
i_{4,k+1} &= \begin{cases} f_4(F_{2,k+1}) & \text{if} \quad F_{2,k+1} < 0, \\ 0 & \text{if} \quad F_{2,k+1} \ge 0, \end{cases}
\end{aligned} \tag{12}$$

where the functions $f_j\ (j = 1,2,3,4)$ are composed by means of the characteristics of the actuator.

The computation algorithm described above is summarized and graphically illustrated in Figure 5.

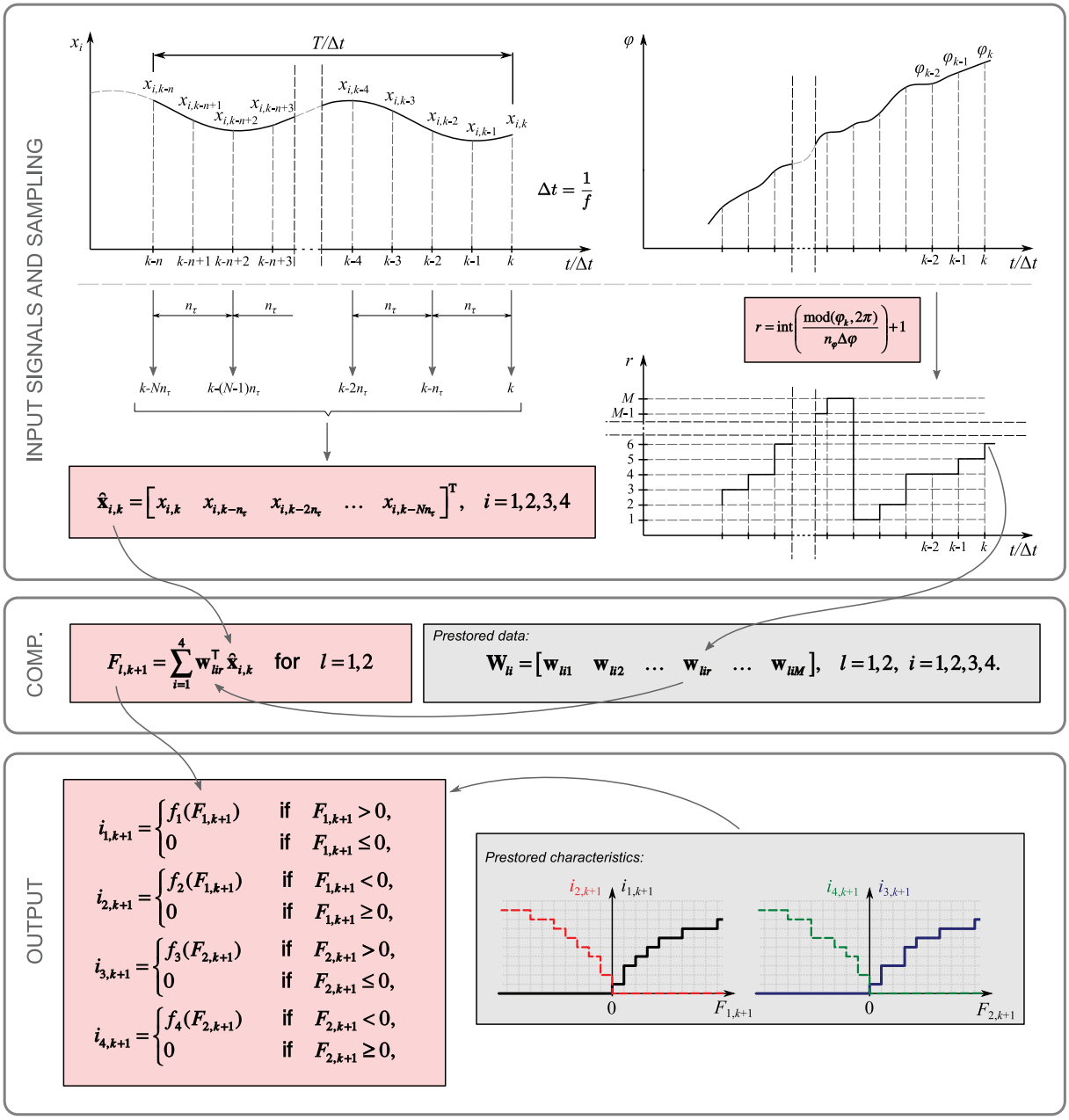

Figure 5: Computation algorithm of the virtual cutting force

4.2 Computation efforts

The computation algorithm should be run in a real time environment with up to 100 kHz sampling frequency. Namely, 0.01 ms is available to generate the cutting force based on the actually measured displacements of the tool. This fact implies very hard requirements against the real target computer. To make these requirements more realistic, the computational efforts required by the algorithm are detailed in this section.

The variables used in the algorithm are summarized in Table 1. The numbers of computational operations are given in Table 2. As the tables show, the memory usage and the numbers of operation depend on $T/\Delta t$ and on the resolutions N and M. The larger these parameters are, the more accurate the HIL test is, and on contrary, the higher the required computational effort is.

Based on theoretical studies on the linear stability of milling, minimal satisfactory and ideal resolutions were determined for the HIL test. For these resolutions, the memory usage and numbers of the computational operations are calculated in Table 3.

Since the numbers of operations are high and the available computation time is very small, linear processors are not applicable to accomplish the HIL test. However, the computation of Eqn. (4) can be parallelized well, and FPGA (Field-Programmable Gate Array) technology based real target systems seem to be an appropriate choice for the computation.

From the point of view of an FPGA based system, the memory usage of the computation is the bottle neck. Nevertheless, the newest generations of FPGA chips offer large enough built-in ram (so-called block ram) to achieve the ideal setup.

The HIL test is planned to be accomplished using two Xilinx Kintex®-7 XC7K410T FPGA chips with high speed analogue input and output interfaces.

Variable	Type	No. stored values
$\mathbf{x}_i$	16 bit	$4\times T/\Delta t$
φ	10 bit	1
$\hat{\mathbf{x}}_i$	16 bit	$4\times(N+1)$
$\mathbf{W}_{li}$	16 bit	$8\times(N+1)\times M$
F_l	16 bit	2
f_j	16 bit	4×256
i_j	8 bit	4

Table 1: Type and number of variables used in the computation algorithm

Formula	Type	No. operations
Eqn. (4)	Multiplication	$2\times 4\times(N+1)$
	Addition	$2\times(4\times(N+1)+4)$

Table 2: Number of computational operations

Setup	$T/\Delta t$	N	M	Mem. (kbit)	No. comp. op.
Min.	200	100	128	1 675	1 684
Sat.	400	200	256	6 626	3 224
Ideal	400	400	512	26 332	6 424

Table 3: Memory storage and number of computational operations for different setups

5 ACTUATOR

The excitation of spindles during rotation is another difficult problem even if a simple FRF is to be determined with frequency sweeping. Commonly used electrodynamic exciters can be attached to a rotating tool with the help of bearing that transfers the force from the exciter to the tool. Unfortunately, the additional dynamics of the bearing can modify the original dynamics of the tool-spindle system.

Thus, the contactless excitation of the tool is desired just as much as the contactless displacement measurement is required. In the literature, only few articles can be found where electrodynamic actuators are developed for the contactless excitation of milling spindles [5][6][7][8].

Here we present a prototype of an actuator, which is similar to the actuators investigated in [5] and [6], only the orientation and locations of the electromagnets seem to be different. Apart of these, the frequency bandwidth of the actuator is also different, namely, it is as high as 100 kHz in our case.

This requires an advanced current control of the electromagnetic coils using up to 1 MHz switching frequencies involving larger dissipation of the switching circuits and extremely critical and difficult measurement of the currents.

The CAD model of the actuator is shown in Figure 6 that is under construction to prove the concept. In this prototype, two E-shaped electromagnets are installed that can be controlled separately. This configuration will enable us to generate a force vector lying in the quadrant that is bounded by the two magnets. Consequently, the prototype will have strong limitations regarding the direction of the generated force.

The final version of the actuator will contain four electromagnets, the inputs of which will require the four outputs presented in the previous section.

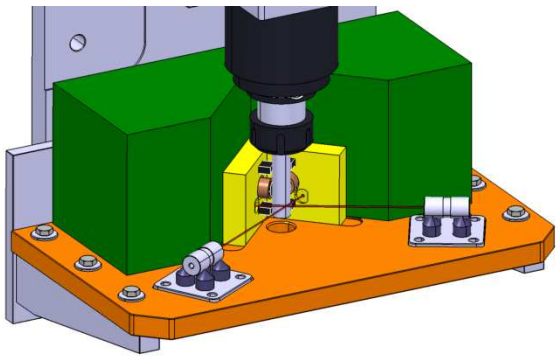

Figure 6: Prototype plan of the actuator

6 CONCLUSION

Three difficult-to-handle aspects of the HIL experiments were discussed in this paper; all of them represent bottle necks in the accomplishment of realistic semi-virtual manufacturing.

A contact-less sensor (Fotonic Beam Reduction (FBR) sensor) was developed to measure the displacements of the tool with high accuracy when the spindle rotates. The computation algorithm was constructed in a way that the cutting force can be calculated with extremely high speed via the sensed present and past positions of the tool. The algorithm was also investigated with respect to the required computational efforts and the required extremely short sampling time. The essential requirements, basic concept and CAD model of an electromagnetic actuator were also presented. The corresponding prototype is under construction, and with the help of this actuator we plan to prove the validity of the HIL concept applied for milling processes.

Although the final assembly of the HIL test and the first experiments are the tasks of future work, the practical experiences on the three intricate parts of HIL test suggest promising results.

7 ACKNOWLEDGMENTS

The research leading to these results has received funding from the European Research Council under the European Union's Seventh Framework Programme (FP/2007-2013) / ERC Advanced Grant Agreement n. 340889.

8 REFERENCES

[1] Stepan, G., Veraszto, Zs., 2016, Digital effects in hardware-in-the-loop experiments of stick-slip phenomena, XXIV ICTAM, Montreal, Canada

[2] Abele, E., Altintas, Y., Brecher, C., 2010, Machine tool spindle units, CIRP Annals - Manufacturing Technology 59(2): 781-802

[3] Zhang, X., Xiong, C., Ding, Y., 2012, Dynamic cutter runout measurement with laser sensor, "Intelligent Robotics and Applications: 5th International Conference, ICIRA 2012, Montreal, Canada, Proceedings, Part II: 264-272

[4] Dombovari, Z., Altintas, Y., Stepan, G., 2010, The effect of serration on mechanics and stability of milling cutters, International Journal of Machine Tools and Manufacture 50(6): 511-520

[5] Matsubaraa, A., Sawamuraa, R., Asanob, K., Murakib, T., 2014, Non-contact measurement of dynamic stiffness of rotating spindle, Procedia CIRP 14: 484–487

[6] Rantataloa, M., Aidanpa, J., Goranssonc, B,. Normand, P., 2007, Milling machine spindle analysis

using FEM and non-contact spindle excitation and response measurement, International Journal of Machine Tools & Manufacture 47: 1034–1045

[7] Mancisidor, X. Beudaert, A. Etxebarria, R. Barcena, J. Munoa, J. Jugo, 2015, Hardware-in-the-loop simulator for stability study in orthogonal cutting, Control Engineering Practice 44: 31-44

[8] Matsubara, A., Tsujimoto, S., Kono, D., 2015, Evaluation of dynamic stiffness of machine tool spindle by non-contact excitation tests, CIRP Annals - Manufacturing Technology, 64(1): 365-368